Glycobiology vol. 15 no. 4 pp. 421–436, 2005
doi:10.1093/glycob/cwi014
Advance Access publication on November 10, 2004

Human EDEM2, a novel homolog of family 47 glycosidases, is involved in ER-associated degradation of glycoproteins

Steven W. Mast[2], Krista Diekman[3], Khanita Karaveg[2], Ann Davis[2], Richard N. Sifers[3], and Kelley W. Moremen[1,2]

[2]Department of Biochemistry and Molecular Biology and Complex Carbohydrate Research Center, University of Georgia, 315 Riverbend Road, Athens, GA 30602-4712, and [3]Departments of Pathology and Molecular and Cellular Biology, Baylor College of Medicine, Houston, TX 77030–3498

Received on October 27, 2004; accepted on November 5, 2004

In the endoplasmic reticulum (ER), misfolded proteins are retrotranslocated to the cytosol and degraded by the proteasome in a process known as ER-associated degradation (ERAD). Early in this pathway, a proposed lumenal ER lectin, EDEM, recognizes misfolded glycoproteins in the ER, disengages the nascent molecules from the folding pathway, and facilitates their targeting for disposal. In humans there are a total of three EDEM homologs. The amino acid sequences of these proteins are different from other lectins but are closely related to the Class I mannosidases (family 47 glycosidases). In this study, we characterize one of the EDEM homologs from *Homo sapiens*, which we have termed EDEM2 (C20orf31). Using recombinantly generated EDEM2, no α-1,2 mannosidase activity was observed. In HEK293 cells, recombinant EDEM2 is localized to the ER where it can associate with misfolded α1-antitrypsin. Overexpression of EDEM2 accelerates the degradation of misfolded α1-antitrypsin, indicating that the protein is involved in ERAD.

Key words: EDEM/EDEM2/ERAD/ER quality control/ mannosidase

Introduction

The biosynthesis and folding of secretory and membrane proteins in the endoplasmic reticulum (ER) is subject to quality control. The ER quality control process can be viewed as having two opposing functions: the correct folding of nascent polypeptides versus the degradation of terminally misfolded intermediates. For the former process, chaperones and folding enzymes facilitate the proper folding and assembly of proteins and oligomeric complexes in the lumen of the ER. Transcription of many of these folding chaperones can be induced by the unfolded protein response (UPR) through an ER-to-nucleus signal transduction pathway. On the latter side of ER quality control, general protein translation can be suppressed by UPR, whereas transcription of the ER-associated degradation (ERAD) machinery is induced, misfolded proteins are prevented from anteriograde transport by retrieval to the ER, and misfolded proteins are eliminated by ERAD or lysosomal/ vacuolar disposal (Ellgaard and Helenius, 2003; Jarosch *et al*., 2003; Kostova and Wolf, 2003; McCracken and Brodsky, 2003; Trombetta and Parodi, 2003).

ERAD is the pathway where terminally misfolded proteins are transported from the ER to the cytosol and are degraded by the proteasome. In mammalian cells, ERAD involves several distinct degradation pathways (Mancini *et al*., 2003; Wu *et al*., 2003). The complexity of the ERAD disposal process is indicated by the demonstration that different pathways may be involved in the elimination of different proteins, different mutations of the same protein may result in different mechanisms for degradation, or the same protein may have alternative fates in different cell types (Cabral *et al*., 2002; Trombetta and Parodi, 2003). In general, ERAD can be viewed in three steps: recognition of the substrate, retrotranslocation to the cytoplasm, and proteolysis (McCracken and Brodsky, 2003). In the first step, chronically misfolded proteins need to be distinguished from folding intermediates. Newly synthesized polypeptides most likely interact with molecular chaperones and folding enzymes, such as the thiol disulfide oxidoreductases. These proteins retain ERAD substrates in the ER, maintain their solubility, and block the formation of disulfide-bonded aggregates. A correlation between substrate release from chaperones and proteasomal degradation has been observed for a number of ERAD substrates (McCracken and Brodsky, 2003).

For glycoproteins, the processing of N-glycans plays a role in quality control (Cabral *et al*., 2001; Yang *et al*., 1998; Yoshida, 2003). Through the opposing actions of glucosidase II and UDP-Glc:glycoprotein glucosyltransferase, glycoprotein folding intermediates can undergo cycles of interaction with the ER lectins calnexin/calreticulin in combination with Erp57 (Ellgaard and Helenius, 2001; McCracken and Brodsky, 2003). Glycoproteins can exit this cycle by either reaching a properly folded conformation, or they can be released from the calnexin cycle for degradation. Interaction with the putative ER lectin, ER degradation–enhancing α-mannosidase-like protein (EDEM), promotes the release of misfolded glycoproteins from calnexin (Molinari *et al*., 2003; Oda *et al*., 2003). A key role in this process is the timing of mannose trimming to the appropriate glycan ligand structure required for EDEM binding. In *Saccharomyces cerevisiae*, evidence suggests that the Man8B isomer, the product of ER α-mannosidase I action, is the glycan signal (Jakob *et al*., 1998). In mammalian cells, oligosaccharide processing is clearly required for ERAD targeting, as indicated by blockage of ERAD

[1]To whom correspondence should be addressed; e-mail: moremen@uga.edu

following treatment with α-mannosidase inhibitors. However, several recent studies suggest that structures other than $Man_8GlcNAc_2$ may act as the glycan signal (Ermonval *et al.*, 2001; Frenkel, *et al.*, 2003; Hosokawa *et al.*, 2003; Kitzmuller *et al.*, 2003).

The components that act in conjunction with EDEM and ER chaperones to mediate retrotranslocation into the cytosol have still not been resolved. Retrotranslocation of ERAD substrates involves components including the translocon, ubiquitination machinery, AAA ATPases (p97 in mammals, Cdc48 in yeast), and cofactors (Ufd1/Npl4), as well as lumenal and cytosolic chaperones (Flierman *et al.*, 2003; Tsai *et al.*, 2002; Ye *et al.*, 2003). Once the glycoprotein is in the cytosol, it can receive polyubiquitin modification that acts as a targeting signal for proteasomal degradation. The glycoprotein is also acted on by a cytosolic glycosyl asparginase to remove the attached oligosaccharide before proteasomal degradation.

Previous work on mouse EDEM and on the *S. cerevisiae* homolog, Htm1p/Mnl1p, has implicated these proteins as lumenal lectins that mediate recognition of unfolded ERAD substrates. In yeast, Htm1p/Mnl1p is localized to the ER and lacks mannosidase activity; its gene deletion resulted in a reduced rate of degradation of misfolded glycoproteins. It was proposed that Htm1p/Mnl1p acts as a $Man_8GlcNAc_2$ binding lectin that initiates glycoprotein ERAD (Jakob *et al.*, 2001; Nakatsukasa *et al.*, 2001). In mammalian cells, EDEM is localized to the ER, interacts with the COOH-terminus of calnexin, lacks mannosidase activity, and is up-regulated by ER stress through XBP1 (Hosokawa *et al.*, 2001; Oda *et al.*, 2003; Yoshida *et al.*, 2003). Overexpression of EDEM accelerates the degradation of misfolded glycoproteins by promoting their release from calnexin, whereas down-regulation of EDEM delays degradation (Molinari *et al.*, 2003; Oda *et al.*, 2003).

In the human genome there are three human EDEM homologs. Human EDEM1 (KIAA0212) is closely related to the previously characterized mouse EDEM. We propose the following nomenclature for the two remaining human homologs. The gene product of chromosome 20 open reading frame 31 (C20orf31), which we call EDEM2, is described in this article. EDEM3 (C1orf22) remains uncharacterized. In the present study, we characterize EDEM2, which also has no α1,2-mannosidase activity but is similar to the other non-catalytic α-mannosidase-like proteins in domain structure and subcellular localization to the ER. Two human genetic variants of α1-antitrypsin (AT), N_{HK} and PI Z, which can lead to emphysema and/or liver cirrhosis (Parfrey *et al.*, 2003) were used as model proteins for the studies on EDEM2. In this article we show that human EDEM2 is expressed in all tissues and is a glycoprotein and direct interaction between EDEM2 and AT mutants is demonstrated by coimmunoprecipitation. Overexpression of full-length EDEM2 accelerates the degradation of the misfolded AT mutants, N_{HK} and PI Z, but not of unglycosylated PI Z. In contrast, overexpression of a COOH-terminal truncated form of EDEM2 containing only the mannosidase-homology domain does not accelerate mutant AT degradation in HEK293 cells. These data indicate that human EDEM2 has a similar function as its homologs, mouse EDEM and yeast Htm1p/Mnl1p, in targeting misfolded glycoproteins for ERAD.

Results

Characteristics of the cDNA sequence

Three human EDEM homologs were found by BLAST searches of EST sequences using the coding regions of family 47 α-mannosidases as query sequences. Based on the nomenclature for mouse EDEM1 (Hosokawa *et al.*, 2001) and its corresponding human EDEM1 ortholog, we have termed the remaining human homologs EDEM2 and EDEM3. The focus of the following study is the characterization of human EDEM2 and its role in ERAD.

The open reading frame of EDEM2 encodes a 578 amino acid (M_r 64,752) protein (Figure 1A) that predicts an NH_2-terminal cleavable signal sequence. Kyte-Doolittle hydropathy analysis (Figure 1B) and analysis of the EDEM2 sequence using the SOSUI program suggest EDEM2 is soluble protein (Hirokawa *et al.* 1998; Kyte and Doolittle, 1982). Four putative Asn-linked glycosylation consensus sites were identified. With the exception of two polymorphisms, our protein sequence matches the NCBI protein reference sequence (GenPept NP_060687). In the corresponding nucleotide sequence (GenBank NM_018217) there are two silent polymorphisms (bp 222 and 270) in addition to two base pair changes (bp 1366 and 1531), which result in protein sequence polymorphisms of A456T and S511C, respectively. Our protein sequence is identical to GenPept BAB14731.1/Swiss-Prot Q9BV94; however, in comparison to the corresponding nucleotide sequence (GenBank accession number AK023931), there is one silent polymorphism at bp 270.

Direct sequence comparison of EDEM2 with other EDEM homologs indicated that the sequence similarity among these proteins is restricted to the regions that have been shown to contain the $(\alpha\alpha)_7$ barrel catalytic domain of the Class I mannosidases (glycosidase family 47) (Figure 1C and 1D) (Vallee *et al.*, 2000a,b). In contrast, outside this region of similarity to the family 47 glycosidase catalytic domain there is limited similarity to other protein sequences (see later discussion) as determined by BLAST searches to NCBI sequence databases. The sequence relationship shared by the EDEM homologs and family 47 glycosidases is shown in Figure 2. Comparison of the entire sequence indicated that human EDEM1 is 92% identical to mouse EDEM, and human EDEM2 is 93% identical to its mouse ortholog (GenPept AAH08268). A mouse homolog of EDEM3 was not found.

Comparing the mannosidase homology domain of the human EDEM homologs, EDEM2 shares 42% and 43% identity with EDEM1 and EDEM3, respectively. Comparatively, EDEM2 shares 32% identity with human ER Man I within the mannosidase-homology domain. Outside of the mannosidase homology domain, the human EDEM homologs are surprisingly not conserved. EDEM1 has a much longer N-terminus before the mannosidase homology domain compared to EDEM2 and EDEM3, which only have a few residues before the mannosidase homology domain (Figure 1D and Table I). The sequences following the mannosidase homology domain are also divergent. The length of the COOH-terminal tail is comparable between EDEM1 and EDEM2, whereas EDEM3 has a considerably longer tail.

(A)

```
-18  TGAGAGGACACGAGCTCTATGCCTTTCCGGCTGCTCATCCCGCTCGGCCTCCTGTGCGCGCTGCTGCCTCAGCACCATGGTGCGCCAGGT
-6                    M  P  F  R  L  L  I  P  L  G  L  L  C  A  L  L  P  Q  H  H  G  A  P  G

73   CCCGACGGCTCCGCGCCAGATCCCGCCCACTACAGGGAGCGAGTCAAGGCCATGTTCTACCACGCCTACGACAGCTACCTGGAGAATGCC
25   P  D  G  S  A  P  D  P  A  H  Y  R  E  R  V  K  A  M  F  Y  H  A  Y  D  S  Y  L  E  N  A

163  TTTCCCTTCGATGAGCTGCGACCTCTCACCTGTGACGGGCACGACACCTGGGGCAGTTTTTCTCTGACTCTAATTGATGCACTGGACACC
55   F  P  F  D  E  L  R  P  L  T  C  D  G  H  D  T  W  G  S  F  S  L  T  L  I  D  A  L  D  T

253  TTGCTGATTTTGGGGAACGTCTCAGAATTCCAAAGAGTGGTTGAAGTGCTCCAGGACAGCGTGGACTTTGATATTGATGTGAACGCCTCT
85   L  L  I  L  G  N  V  S  E  F  Q  R  V  V  E  V  L  Q  D  S  V  D  F  D  I  D  V  N  A  S

343  GTGTTTGAAACAAACATTCGAGTGGTAGGAGGACTCCTGTCTGCTCATCTGCTCTCCAAGAAGGCTGGGGTGGAAGTAGAGGCTGGATGG
115  V  F  E  T  N  I  R  V  V  G  G  L  L  S  A  H  L  L  S  K  K  A  G  V  E  V  E  A  G  W

433  CCCTGTTCCGGGGCCTCTCCTGAGAATGGCTGAGGAGGCGGCCCGAAAACTCCTCCCAGCCTTTCAGACCCCCACTGGCATGCCATATGGA
145  P  C  S  G  P  L  L  R  M  A  E  E  A  A  R  K  L  L  P  A  F  Q  T  P  T  G  M  P  Y  G

523  ACAGTGAACTTACTTCATGGCGTGAACCCAGGAGAGACCCCTGTCACCTGTACGGCAGGGATTGGGACCTTCATTGTTGAATTTGCCACC
175  T  V  N  L  L  H  G  V  N  P  G  E  T  P  V  T  C  T  A  G  I  G  T  F  I  V  E  F  A  T

613  CTGAGCAGCCTCACTGGTGACCCGGTGTTCGAAGATGTGGCCAGAGTGGCTTTGATGCGCCTCTGGGAGAGCCGGTCAGATATCGGGCTG
205  L  S  S  L  T  G  D  P  V  F  E  D  V  A  R  V  A  L  M  R  L  W  E  S  R  S  D  I  G  L

703  GTCGGCAACCACATTGATGTGCTCACTGGCAAGTGGGTGGCCCAGGACGCAGGCATCGGGGCTGGCGTGGACTCCTACTTTGAGTACTTG
235  V  G  N  H  I  D  V  L  T  G  K  W  V  A  Q  D  A  G  I  G  A  G  V  D  S  Y  F  E  Y  L

793  GTGAAAGGAGCCATCCTGCTTCAGGATAAGAAGCTCATGGCCATGTTCCTAGAGTATAACAAAGCCATCCGGAACTACACCCGCTTCGAT
265  V  K  G  A  I  L  L  Q  D  K  K  L  M  A  M  F  L  E  Y  N  K  A  I  R  N  Y  T  R  F  D

883  GACTGGTACCTGTGGGTTCAGATGTACAAGGGGACTGTGTCCATGCCAGTCTTCCAGTCCTTGGAGGCCTACTGGCCTGGTCTTCAGAGC
295  D  W  Y  L  W  V  Q  M  Y  K  G  T  V  S  M  P  V  F  Q  S  L  E  A  Y  W  P  G  L  Q  S

973  CTCATTGGAGACATTGACAATGCCATGAGGACCTTCCTCAACTACTACACTGTATGGAAGCAGTTTGGGGGGCTCCCGGAATTCTACAAC
325  L  I  G  D  I  D  N  A  M  R  T  F  L  N  Y  Y  T  V  W  K  Q  F  G  G  L  P  E  F  Y  N

1063 ATTCCTCAGGGATACACAGTGGAGAAGCGAGAGGGCTACCCACTTCGGCCAGAACTTATTGAAAGCGCAATGTACCTCTACCGTGCCACG
355  I  P  Q  G  Y  T  V  E  K  R  E  G  Y  P  L  R  P  E  L  I  E  S  A  M  Y  L  Y  R  A  T

1153 GGGGATCCCACCCTCCTAGAACTCGGAAGAGATGCTGTGGAATCCATTGAAAAAATCAGCAAGGTGGAGTGCGGATTTGCAACAATCAAA
385  G  D  P  T  L  L  E  L  G  R  D  A  V  E  S  I  E  K  I  S  K  V  E  C  G  F  A  T  I  K

1243 GATCTGCGAGACCACAAGCTGGACAACCGCATGGAGTCGTTCTTCCTGGCCGAGACTGTGAAATACCTCTACCTCCTGTTTGACCCAACC
415  D  L  R  D  H  K  L  D  N  R  M  E  S  F  F  L  A  E  T  V  K  Y  L  Y  L  L  F  D  P  T

1333 AACTTCATCCACAACAATGGGTCCACCTTCGACGCGGTGATCACCCCCTATGGGGAGTGCATCCTGGGGGCTGGGGGGTACATCTTCAAC
445  N  F  I  H  N  N  G  S  T  F  D  A  V  I  T  P  Y  G  E  C  I  L  G  A  G  G  Y  I  F  N

1423 ACAGAAGCTCACCCCATCGACCCTGCCGCCCTGCACTGCTGCCAGAGGCTGAAGGAAGAGCAGTGGGAGGTGGAGGACTTGATGAGGGAA
475  T  E  A  H  P  I  D  P  A  A  L  H  C  C  Q  R  L  K  E  E  Q  W  E  V  E  D  L  M  R  E

1513 TTCTACTCTCTCAAACGGAGCAGGTCGAAATTTCAGAAAAACACTGTTAGTTCGGGGCCATGGGAACCTCCAGCAAGGCCAGGAACACTC
505  F  Y  S  L  K  R  S  R  S  K  F  Q  K  N  T  V  S  S  G  P  W  E  P  P  A  R  P  G  T  L

1603 TTCTCACCAGAAAACCATGACCAGGCAAGGGAGAGGAAGCCTGCCAAACAGAAGGTCCCACTTCTCAGCTGCCCCAGTCAGCCCTTCACC
535  F  S  P  E  N  H  D  Q  A  R  E  R  K  P  A  K  Q  K  V  P  L  L  S  C  P  S  Q  P  F  T

1693 TCCAAGTTGGCATTACTGGGACAGGTTTTCCTAGACTCCTCATAA
565  S  K  L  A  L  L  G  Q  V  F  L  D  S  S  *
```

Fig. 1. EDEM2 sequence and comparison with other Class 1 mannosidases and mannosidase-like proteins. (**A**) cDNA and protein sequences of EDEM2 are shown. Highlighted on the protein sequence are the following: predicted cleavable signal sequence (underscored), mannosidase homology domain (boldface), the four potential N-glycosylation sites (triangles), and four positions of sequence polymorphisms are noted. All four polymorphisms are different from GenBank NM_018217 (two silent and two nonconservative substitutions, asterisk), whereas only one silent polymorphism is found in comparison to GenBank AK023931 (diamond).

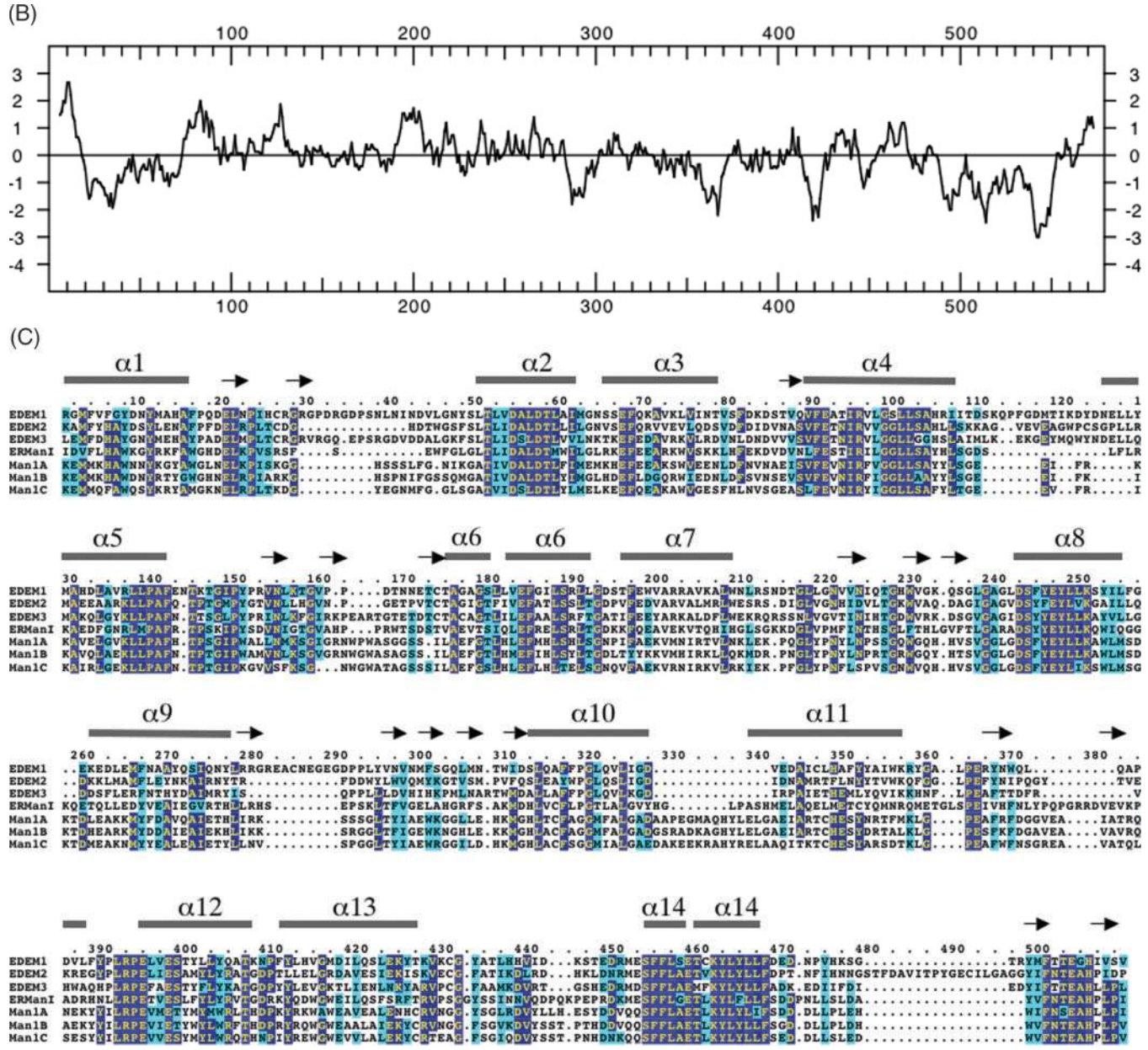

Fig. 1. (Continued) (**B**) Kyte-Doolittle hydropathy plot for EDEM2. (**C**) Alignment of human EDEM homologs with representative sequences of the catalytic domains of the family 47 glycosidases. The multiple sequence alignment generated by Clustal W contains the catalytic core of *H. sapiens* members of the Class I mannosidases for comparison to the EDEM homologs: EDEM1 (GenPept CAC69370); EDEM2 (GenPept NP_060687); EDEM3 (GenPept NP_079467); ER mannosidase I (ER ManI, GenPept NP_057303); Golgi mannosidase IA (ManIA, GenPept NP_005898); Golgi mannosidase IB (ManIB, GenPept NP_006690); Golgi mannosidase IC (ManIC, GenPept NP_065112). Identical residues are shaded dark blue, whereas similar residues are shaded light blue. Using the crystal structure of human ER mannosidase I (Vallee *et al.*, 2000a), the positions of the α helices are represented by bars, and βsheets are shown by arrows. The alignment includes amino acid residues 39–482 of EDEM2.

Tissue distribution of mRNA transcripts for EDEM2

Transcript levels were determined by northern blot analysis using a 1 kb polymerase chain reaction (PCR) amplimer from the coding region as a radiolabeled probe. A transcript of ~ 2 kb was found in all tissues (Figure 3), in agreement with the size of the transcript predicted from the full-length cDNA (1734 bp). The transcript was uniformly expressed in most tissues, but brain and skeletal muscles had lower transcript levels and small intestine and peripheral blood leukocytes had slightly higher levels.

Recombinant protein expression in HEK293 cells

Epitope-tagged constructs were prepared to examine the localization and function of EDEM2 in mammalian cells. In the first construct (*T. cruzi* lysosomal α-mannosidase [TCM]-EDEM2/pEAK), the putative NH_2-terminal signal sequence (amino acids 1–17) was replaced with the cleavable signal sequence of the *Trypanosoma cruzi* α-mannosidase (Vandersall-Nairn *et al.*, 1998). This construct also contained a His tag and hemagglutinin (HA) epitope at the NH_2-terminus between the TCM-signal sequence and the

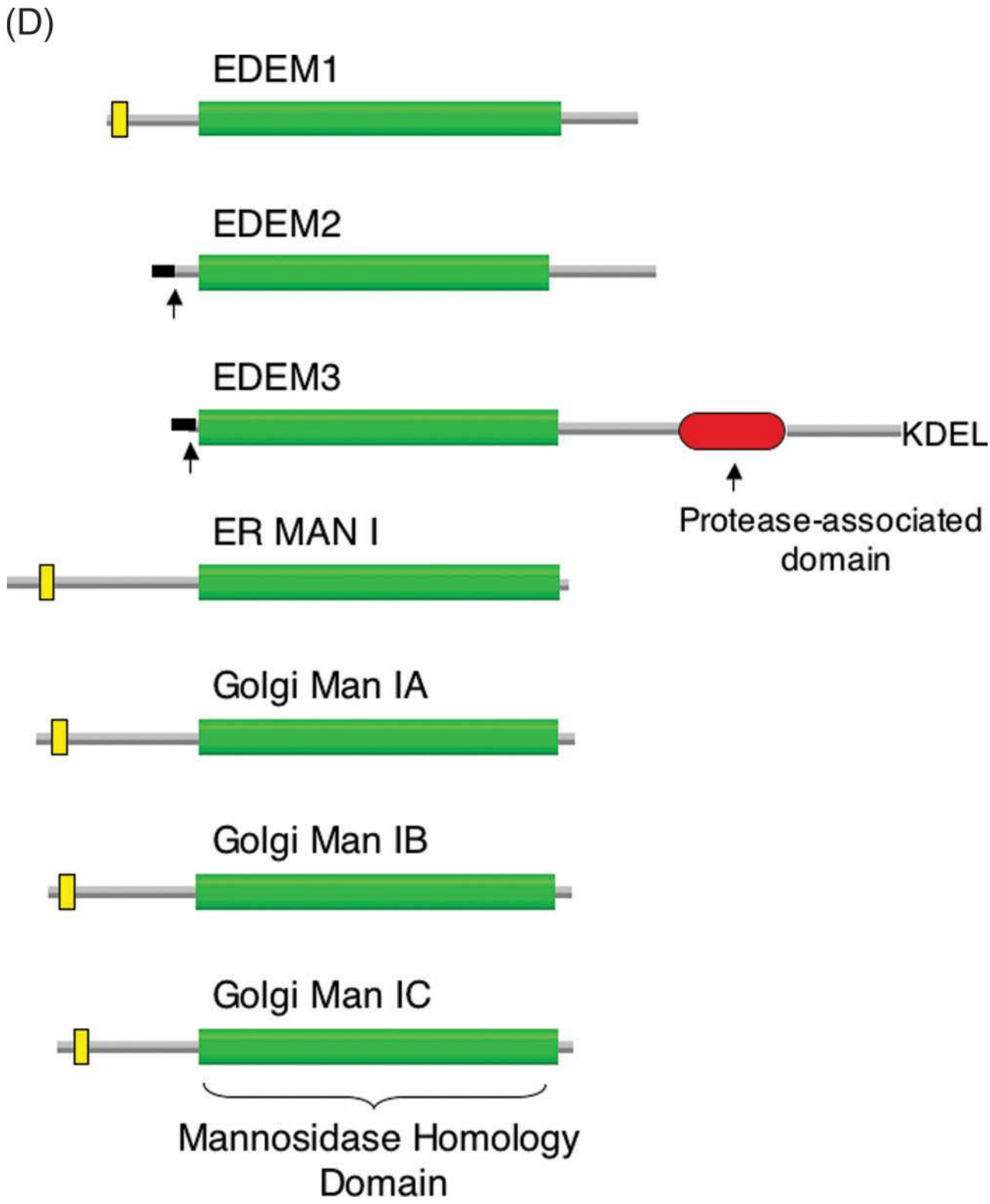

Fig. 1. (Continued) (**D**) Cartoon representation of the full-length protein sequences depicted in **C**. The mannosidase homology domain is shown in green, the protease-associated domain is red, the signal sequence is black, the transmembrane domain is yellow, and other sequences are gray. Putative signal sequence cleavage site is indicated by the arrow.

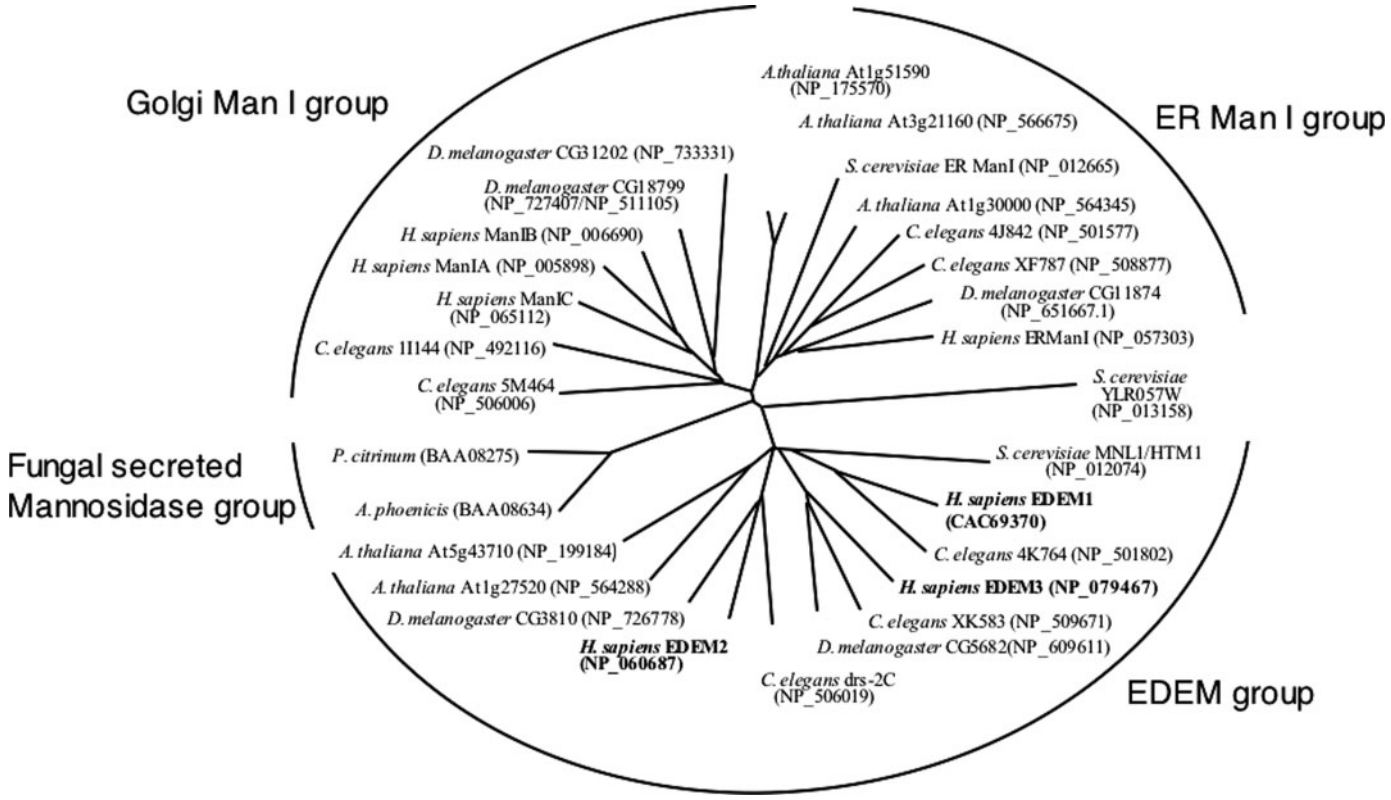

Fig. 2. Dendrogram for selected members of the Class 1 mannosidase family displayed as a radial unrooted tree. Where complete genome sequences were present, all known members from human, *Drosophila*, *C. elegans*, *Arabidopsis*, and selected fungal sources were chosen. The sequences are divided into four groups, ER mannosidase I, Golgi mannosidase I, fungal secreted mannosidase, and EDEM. Sequences were edited to compare the conserved α-mannosidase catalytic core domain of the family. The GenPept numbers are noted in parentheses.

Table I. Comparison of domain lengths for family 47 glycosidases

Human homologs	NH_2 extension[a]	Mannosidase-homology domain	COOH-extension
EDEM1	134	452	71
EDEM2	39	443	96
EDEM3	13	442	434
ER Man I	253	442	4
Golgi Man1A	199	441	13
Golgi Man1B	184	442	15
Golgi Man1C	178	439	13

[a]Including cytoplasmic tails, transmembrane domains, stem regions, or cleaved signal sequences in the relevant proteins.

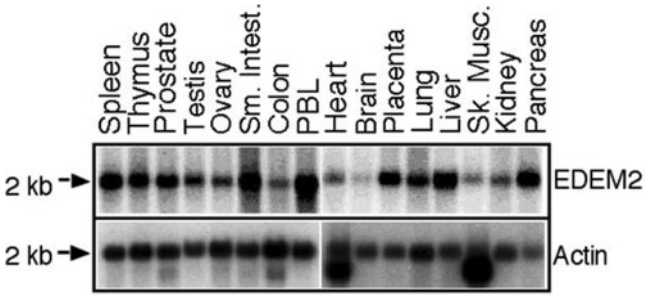

Fig. 3. Tissue distribution of mRNA transcripts. A northern blot of human poly(A+) RNAs was hybridized with radiolabeled probes generated from a 1-kb PCR amplimer from the coding region of EDEM2. The blot was rehybridized with β-actin cDNA as a control. The size of the transcripts indicated was estimated based on the electrophoretic mobility of radiolabeled RNA standards. PBL, peripheral blood leukocytes.

EDEM2 coding region. As a control for the expression and localization of the NH_2-terminal-tagged protein, a COOH-terminal-tagged construct was also generated, retaining the endogenous NH_2-terminal signal sequence. This construct (EDEM2-Myc-HA-His/pEAK) contained the full-length EDEM2 coding region with a Myc-HA-His tag as a fusion protein at the COOH-terminus.

HEK293 cells were independently transfected with the constructs and were either directly characterized as transient transfectants or subjected to antibiotic selection to generate stably expressing cell lines. The recombinant protein was either purified by Ni^{2+}-nitrilotriacetic acid (NTA) chromatography from detergent cell extracts, or characterized by biosynthetic labeling with [^{35}S]-Met/Cys and immunoprecipitation (IP) from the labeled cell extracts. In radiolabeled cell extracts or Ni^{2+}-NTA purified, unlabeled material of either NH_2– or COOH-tagged forms of EDEM2, an apparent molecular mass of ~ 70 and 71 kDa was observed by

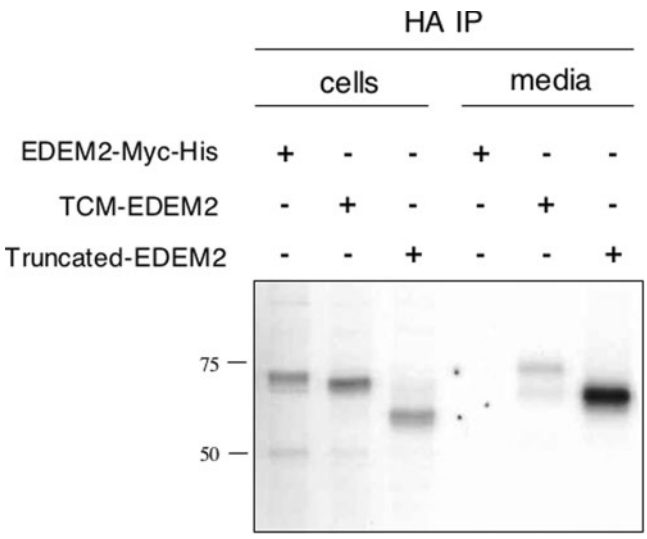

Fig. 4. COOH-terminal truncation leads to increased secretion of EDEM2. HEK293 cells stably transfected with TCM-EDEM2/pEAK, EDEM2-Myc-HA-His/pEAK, or truncated EDEM2/pEAK were radiolabeled for 2 h with [^{35}S]-Met/Cys and chased for 3 h. Equivalent amounts of cell lysates and media were immunoprecipitated with antibody to the HA epitope, and the samples were separated by SDS–PAGE and detected by autoradiography. In the cells, an apparent molecular mass of 71 kDa, 70 kDa, and 64 kDa was observed for EDEM2-Myc-HA-His, TCM-EDEM2, and truncated EDEM2, respectively. Levels of secreted protein were compared to the levels of intracellular protein by densitometry. EDEM2-Myc-HA-His was not secreted. Truncated EDEM2 had 2.6 times more protein in the media compared to intracellular levels of truncated EDEM2, and TCM-EDEM2 had 0.64 times as much protein in the media compared to intracellular levels of TCM-EDEM2.

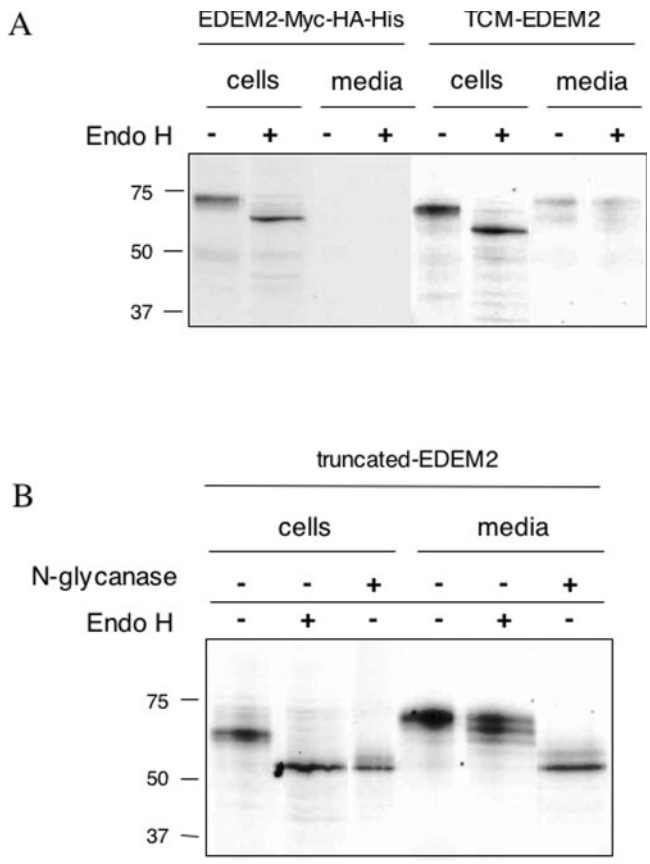

Fig. 5. Glycosidase digestion of EDEM2. HEK293 cells stably transfected with TCM-EDEM2/pEAK, EDEM2-Myc-HA-His/pEAK, or truncated EDEM2/pEAK were radiolabeled for 2 h with [^{35}S]-Met/Cys and chased for 3 h. After IP from cell lysates or media, (**A**)TCM-EDEM2, EDEM2-Myc-HA-His and (**B**) truncated EDEM2 were digested by endoglycosidase H or N-glycanase and resolved by SDS–PAGE. In cell lysates, all of the EDEM2 constructs were sensitive to endoglycosidase H digestion; however, EDEM2 forms that were secreted into the media became predominantly endoglycosidase H insensitive, indicating conversion to complex type structures during secretion.

sodium dodecyl sulfate–polyacrylamide gel electrophoresis (SDS–PAGE), respectively (Figure 4). These size differences are consistent with the differences in lengths of the epitope tags appended to the coding regions.

A truncated EDEM2 construct, corresponding to amino acid position 18 to 492 of EDEM2, was also generated from the TCM-EDEM2/pEAK construct. The truncated construct does not contain the COOH-terminal extension beyond the mannosidase homology domain. In immunoprecipitates from radiolabeled HEK293 cell extracts (Figure 4) or from Ni^{2+}-NTA purified unlabeled material, a 64-kDa protein was detected. Truncated EDEM2 was found both intracellularly and in the media, in contrast to the predominantly intracellular location of TCM-EDEM2 (Figure 4). Thus, the COOH-terminal polypeptide extension beyond the α-mannosidase homology domain plays a role in ER retention of EDEM2.

Glycosylation of EDEM2

In EDEM2 immunoprecipitates of the cell lysate, digestion with N-glycanase or endoglycosidase H resulted in a shift in apparent molecular mass of the full length constructs from ~ 70 kDa to ~ 64 kDa, whereas truncated EDEM2 shifted from ~ 64 to 58 kDa (Figure 5). The sensitivity of the N-glycans to cleavage by endoglycosidase H indicated that the oligosaccharides were still high-mannose type and that the glycoprotein had likely not reached the Golgi complex. The material that was secreted into the media exhibited a slightly larger size than the intracellular form, suggesting that glycan modification had occurred in the Golgi during transit. The secreted material was only partially sensitive to digestion by endoglycosidase H but completely sensitive to digestion by N-glycanase. After digestion by N-glycanase, intracellular and secreted EDEM2 had the same electrophoretic mobility, indicating the difference in size of the glycosylated proteins can be accounted for by differences in glycosylation.

Assay for α-1,2 mannosidase activity

To determine if EDEM2 has α-1,2 mannosidase activity, TCM-EDEM2 was purified from cell extracts by Ni^{2+}-NTA chromatography and was incubated with $Man_9GlcNAc_2$-$Man_5GlcNAc_2$-pyridylamine (PA) tagged substrates. The oligosaccharides were analyzed by NH_2-high-performance liquid chromatography (HPLC), and no changes in retention time were detected for any of the digestion products (Figure 6A). In contrast, a similar amount of recombinant

ER mannosidase I (Gonzalez *et al.*, 1999) or Golgi mannosidase IA (Lal *et al.*, 1998) each could trim the substrates to their expected digestion products.

In an additional step to determine if EDEM2 has α-1,2 mannosidase activity, cells were metabolically labeled with [^{3}H]mannose, and the N-linked oligosaccharide profile was determined for glycoproteins isolated from cells transfected with EDEM2 versus untransfected cells. First, lipid-linked oligosaccharides were removed from the cell extracts by acetone precipitation, and then N-linked oligosaccharides were released from the glycoprotein fraction by endoglycosidase H digestion. The [^{3}H]-labeled oligosaccharides were then PA-tagged to allow comparison with the PA-tagged high-mannose standards. In both untransfected cells and in cells overexpressing EDEM2, peaks eluting with the retention time of $Glc_1Man_9GlcNAc$ and $Man_9GlcNAc$ accounted for the majority of the labeled oligosaccharide (Figure 6B). No difference was observed in the oligosaccharide profile between untransfected and EDEM2 transfected cell extracts labeled with a 30-min pulse of [^{3}H]mannose or a 30-min pulse and 30-min chase, indicating EDEM2 has no effect on the rate of N-glycan processing. These data are consistent with the lack of α-1,2 mannosidase activity for other EDEM homologs, *S.cerevisiae* Htm1p/Mnl1p and murine EDEM (Hosokawa *et al.*, 2001; Jakob *et al.*, 2001; Nakatsukasa *et al.*, 2001).

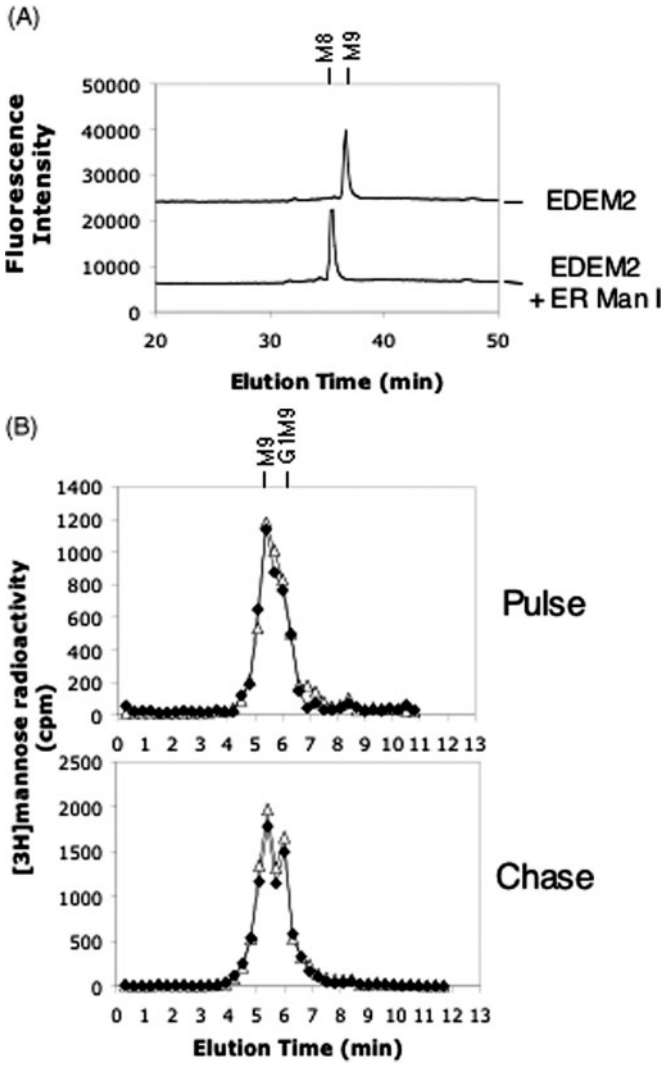

Fig. 6. Test of α-mannosidase activity for EDEM2 in vitro and in HEK293 cells. (**A**)$Man_{9-5}GlcNAc_2$-PA tagged oligosaccharides were incubated with Ni^{2+}-NTA purified EDEM2 for varied times (see *Materials and methods*). Comparison of α-1,2 mannosidase activity for purified EDEM2 is shown in the top panel and EDEM2 mixed with ER mannosidase I is shown in the lower panel. Both reactions were assayed using the $Man_9GlcNAc_2$-PA substrate. Oligosaccharides were resolved by NH_2-HPLC. M9 and M8 ($Man_{9-8}GlcNAc_2$) correspond to the positions of the standards. No change in elution time for the $Man_9GlcNAc_2$-PA substrate is seen for the EDEM2 sample, whereas the sample with the added ER mannosidase I shows a change in the mobility to $Man_8GlcNAc_2$-PA (**B**)Cells stably coexpressing TCM-EDEM2/pEAK and PI Z/pcDNA3.1 (open triangles) or expressing PI Z/pcDNA3.1 alone (solid diamonds) were radiolabeled with [^{3}H]mannose for 30 min and chased for 30 min. Total N-linked glycoproteins were isolated, and the oligosaccharides were released by endoglycosidase H digestion and separated by HPLC. The positions of the standards are shown at the top of the figure. G1M9 corresponds to $Glc_1Man_9GlcNAc_1$ and M9 corresponds to $Man_9GlcNAc_1$.

Immunolocalization of an epitope-tagged form of EDEM2 in transfected cells

The subcellular localization of EDEM2 was determined by the stable transfection of the TCM-EDEM2/pEAK construct into HEK293 cells followed by detection of the HA epitope tag by indirect immunofluorescence (IF). Double staining of the cells was accomplished by the use of a mouse monoclonal anti-HA antibody and a rabbit polyclonal anti-calreticulin antibody, detected by the fluorphore conjugated secondary antibodies. The IF pattern of TCM-EDEM2 was broadly distributed throughout the cytoplasm in a reticular pattern (Figure 7, row A). Colocalization of EDEM2 and calreticulin was observed. Untransfected cells showed no detectable fluorescence. No similarity in localization was detected between TCM-EDEM2 and the cytosolic proteins MEK-1 or cytosolic α-mannosidase (Figure 7, row B). Comparing TCM-EDEM2 with the Golgi marker protein Golgi α-mannosidase II, the IF pattern was not similar, although some limited overlap could be detected (Figure 7, row C). When the cell line expressing truncated EDEM2 was examined, a similar colocalization with calreticulin was revealed (Figure 7, row D). The overlay was not completely identical, likely as a result of the increased intensity of the signal. Truncated EDEM2 did not colocalize with the Golgi or cytosolic markers (Figure 7, rows E and F). These data indicate that full-length EDEM2 is localized in the ER and that the portion of truncated EDEM2 that had not yet been secreted was also retained mostly within the ER.

Using the COOH-terminally tagged EDEM2-Myc-His/pEAK construct with anti-Myc and anti-calreticulin antibodies, a colocalization pattern was observed (Figure 7, row G) similar to the NH_2-terminal tagged form indicating that neither tag influences the ER retention of the protein.

IP of EDEM2 with AT variants

To determine whether EDEM2 is able to interact with ERAD substrates, HEK293 cells were cotransfected with EDEM2 and mutant forms of AT. The N_{HK} and PI Z

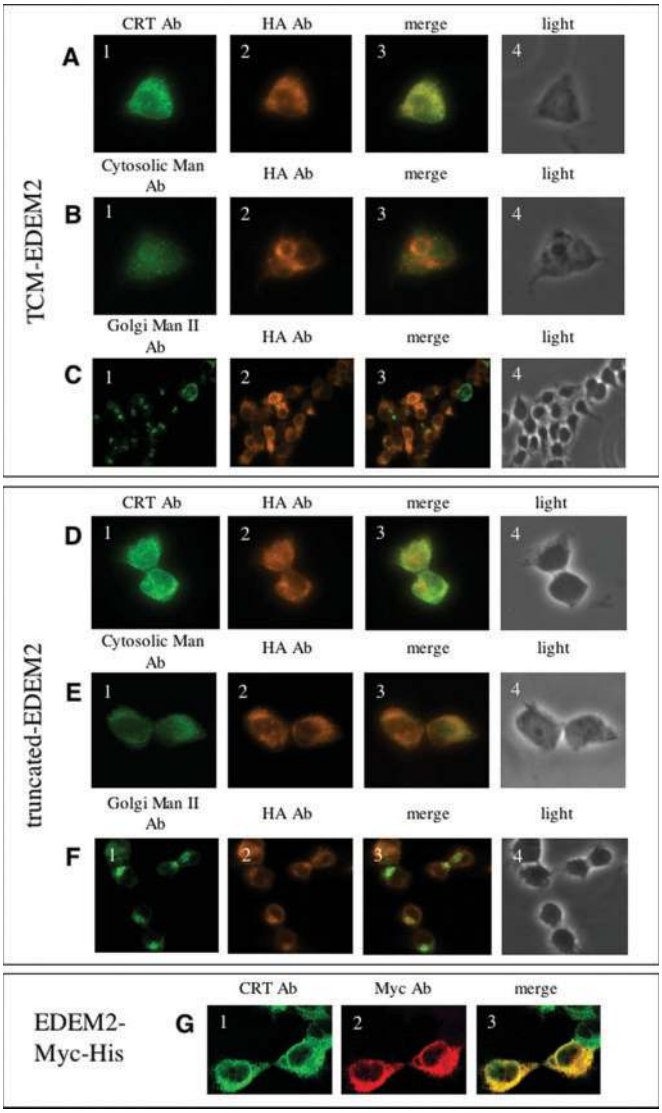

Fig. 7. IF studies on HEK293 cells stably transfected with EDEM2. Tagged forms of EDEM2 colocalized with the ER marker protein in transfected cells, but not with cytosolic or Golgi marker proteins. TCM-EDEM2 localization is shown in rows A–C, truncated EDEM2 is shown in rows D–F, and the COOH-terminal tagged EDEM2-Myc-His is shown in row G. The ER marker protein, calreticulin, was detected using an anti-rabbit calreticulin antibody (CRT) followed by Alexafluor 488 anti-rabbit secondary antibody (rows A, D, and G; panel 1). Localization of the cytosolic marker, cytosolic α-mannosidase, was detected using an anti-rabbit cytosolic α-mannosidase antibody followed by Alexafluor 488 anti-rabbit secondary antibody (rows B and E; panel 1). Localization of the Golgi was detected using an anti-rabbit Golgi mannosidase II antibody followed by Alexafluor 488 anti-rabbit secondary antibody (rows C and F; panel 1). TCM-EDEM2 and truncated EDEM2 were detected using an anti-mouse HA antibody followed by Alexafluor 594 anti-mouse secondary antibody (rows A–F; panel 2). EDEM2-Myc-His was detected using an anti-mouse Myc antibody followed by Alexafluor 594 anti-mouse secondary antibody (row G; panel 2). Merged view of panels 1 and 2 for each row is shown in panel 3 of the corresponding row. An overlap of fluorescence is indicated by yellow. Panel 4 in all rows shows the equivalent light microscopy images for the cells in panels 1–3.

variants are each retained in the ER prior to their degradation by the proteasome, although some PI Z is able to be secreted from HEK293 cells (Cabral *et al.*, 2002). Data demonstrating an association between EDEM2 and PI Z are shown in Figure 8, and similar results were obtained for the N_{HK} variant (data not shown). IP of TCM-EDEM2 from [^{35}S]-Met/Cys labeled extracts with the antibody to the HA epitope resulted in the coimmunoprecipitation of proteins similar in size to PI Z (Figure 8A). Elution from the protein A-Sepharose resin and subsequent IP with an antibody to AT, confirmed that the corresponding bands were indeed AT (Figure 8B). In the opposite direction, sequential IP of AT followed by elution and reprecipitation with anti-HA antibody resulted in detection of EDEM2 (Figure 8C). Control IPs containing no primary antibodies resulted in no specific secondary IP products, and cells not expressing epitope tagged EDEM2 also resulted in no detection of secondary IP products.

In support of these data, IP from unlabeled cell extracts followed by immunoblotting also detected an association between EDEM2 and mutant forms of AT. Thus, AT could be detected in immunoblots following IP of EDEM2 from cell extracts using the HA antibody (Figure 8D). These data indicate that a complex between the AT variants and recombinant EDEM2 was formed, and the epitope tag did not interfere with the interaction.

Degradation of AT

In HEK293 cells, TCM-EDEM2 or truncated EDEM2 was transiently cotransfected with N_{HK}, PI Z, nonglycosylated PI Z, or a β-galactosidase control construct. In these transfections, a threefold range of EDEM2 expression constructs was used, and no change in AT turnover was observed (data not shown). Previous work has also shown that the rate of mutant AT degradation is not significantly altered as a function of transfection levels, and a high level of AT expression does not saturate any retention or degradation pathways (Cabral *et al.*, 2000, 2002; Liu *et al.*, 1999). To examine the effect of EDEM2 on degradation, HEK293 cells were pulse labeled with [^{35}S]-Met, chased with unlabeled media for up to 5 h, and AT was immunoprecipitated from the media and cell lysates. During the chase, there was a slight shift in the mobility of intracellular AT variants to a lower apparent molecular mass, indicating that glycan trimming had occurred (Figure 9A).

In cells that were not transfected with EDEM2, misfolded AT variants (N_{HK} and PI Z) were retained in the cell for 3 h and then decreased in amount by the 5 h time point (Figure 9A). For the PI Z variant, some AT was able to fold properly and be secreted, but the majority was retained intracellularly and was slowly degraded. On overexpression of TCM-EDEM2, N_{HK} was stable at the 1 h chase time point but was mostly degraded by 3 h (Figure 9A). On overexpression of TCM-EDEM2, PI Z was also stable at the 1 h chase time point, with reduced radiolabeled protein by the 3 h time point and reduced secretion of PI Z.

In cells that were transfected with the nonglycosylated PI Z variant, PI Z(NOG), overexpression of TCM-EDEM2 did not alter the rate of disposal of nonglycosylated PI Z compared to the β-gal control (Figure 9B). In contrast to PI Z, no shift in mobility was detected for PI Z(NOG) (comparing Figures 9A and 9B), as expected for a nonglycosylated protein.

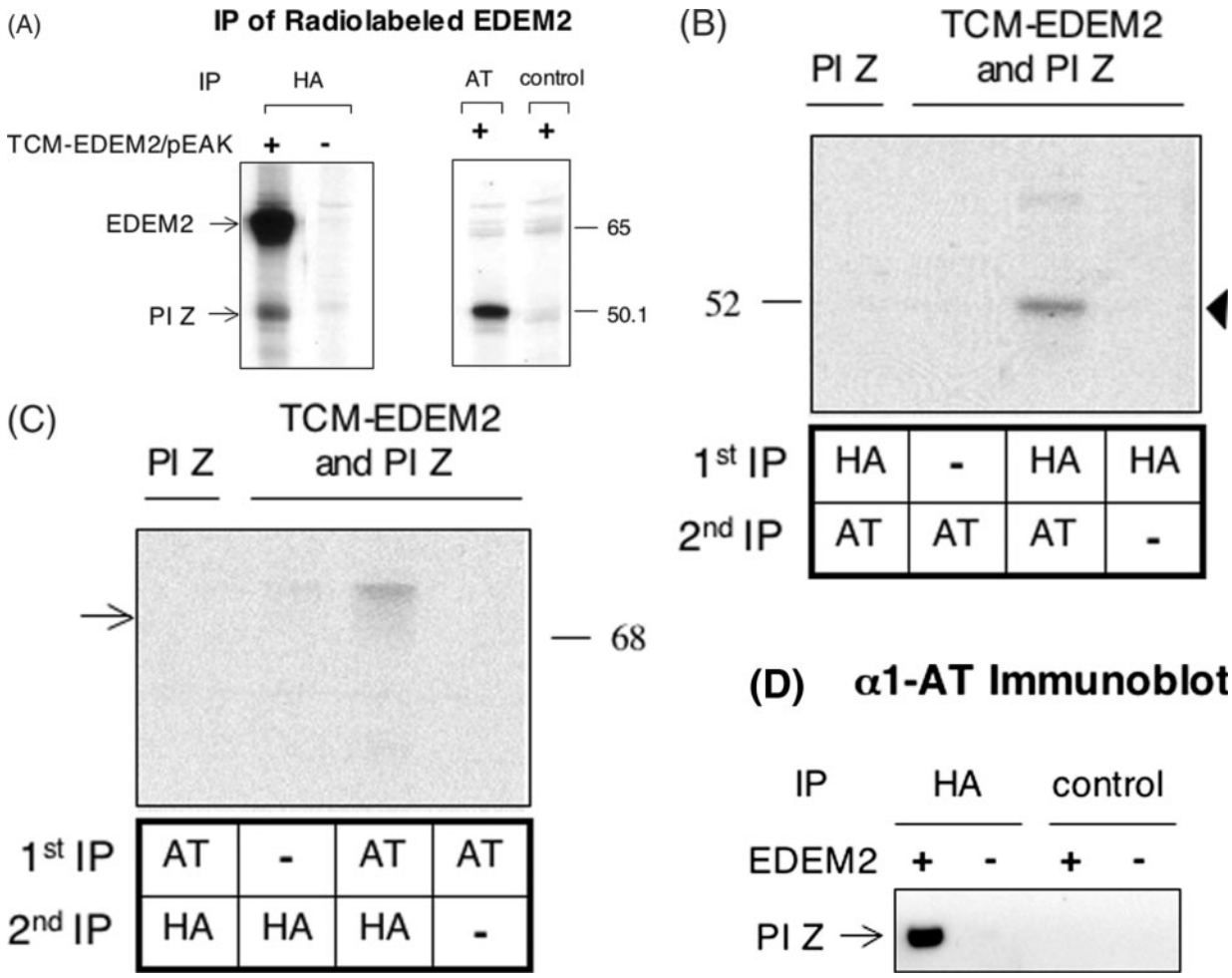

Fig. 8. EDEM2 interacts with AT variant PI Z. (**A**) HEK293 cells coexpressing HA-tagged TCM-EDEM2/pEAK and PI Z/pcDNA3.1 or expressing PI Z/pcDNA3.1 alone were radiolabeled with [^{35}S]-Met/Cys for 2 h. Cell lysates were immunoprecipitated with antibodies to HA, AT, or cdc2 (control). Cross-reacting material with the anti-HA antibody could be seen both at the mobility of the HA-tagged EDEM2 as well as at the mobility of PI Z only in cells stably transfected with both EDEM2 and PI Z indicating an association of PI Z with the HA-tagged EDEM2. (**B**) HEK293 cells stably transfected with PI Z/pcDNA3.1 with or without TCM-EDEM2/pEAK were radiolabeled with [^{35}S]-Met/Cys for 2 h. In a sequential IP, lysates were immunoprecipitated first with the antibody to the HA epitope, then the samples were eluted and immunoprecipitated with the antibody to AT. In the indicated lanes, the antibody was omitted from either the primary or secondary IP. The filled triangle points to the position of AT. The coprecipitating PI Z band was found only in cells expressing EDEM2 and PI Z and only when EDEM2 was immunoprecipitated prior to the PI Z IP. (**C**) Sequential IP, similar to **B**, except that the first IP was with the antibody to AT and the second IP was with the anti-HA antibody. The arrow points to the position of EDEM2. As in **B**, coimmunoprecipitation was only found in cells that coexpressed both TCM-EDEM2 and mutant AT and required the prior IP of the corresponding binding partner. (**D**) In HEK 293 cells co-transfected with both TCM-EDEM2/pEAK and PI Z/pcDNA3.1 or PI Z/pcDNA3.1 alone, TCM-EDEM2 was immunoprecipitated from the cell lysate with the antibody to HA or nonspecific monoclonal antibody control (cdc2), resolved by SDS–PAGE, and then immunoblotted with the antibody to AT. AT cross-reactive material was only visible in blots from cells coexpressing EDEM2 and PI Z and only when the cell extracts were immunoprecipitated with the HA antibody but not a nonspecific control antibody.

Overexpression of truncated EDEM2 did not accelerate degradation of N_{HK} or PI Z, compared with the β-gal controls (Figure 9C). These data suggest that EDEM2 is involved in the disposal of unfolded glycoproteins but not nonglycosylated proteins. Additionally, the COOH-terminal extension beyond the mannosidase-homology domain is essential for the function of EDEM2 in ERAD.

Discussion

We have cloned, expressed, and characterized a human cDNA encoding EDEM2, a protein that is similar in sequence to Class I mannosidases (family 47 glycosidases) (Figures 1 and 2). EDEM2 is a ubiquitously expressed (Figure 3), ER-localized (Figure 7) member of the EDEM subfamily, which is conserved throughout eukaryotic organisms. EDEM2 interacts with mutant forms of AT, N_{HK} and PI Z (Figure 8), and overexpression of EDEM2 accelerates the degradation of the misfolded AT variants (Figure 9) indicating that EDEM2 plays a role in ERAD, similar to the role of mouse EDEM.

The sequence relationship shared by the EDEM homologs exists only in the mannosidase homology domain (Figure 1C). They each have variable NH_2- and COOH-terminal extensions that do not share sequence similarity

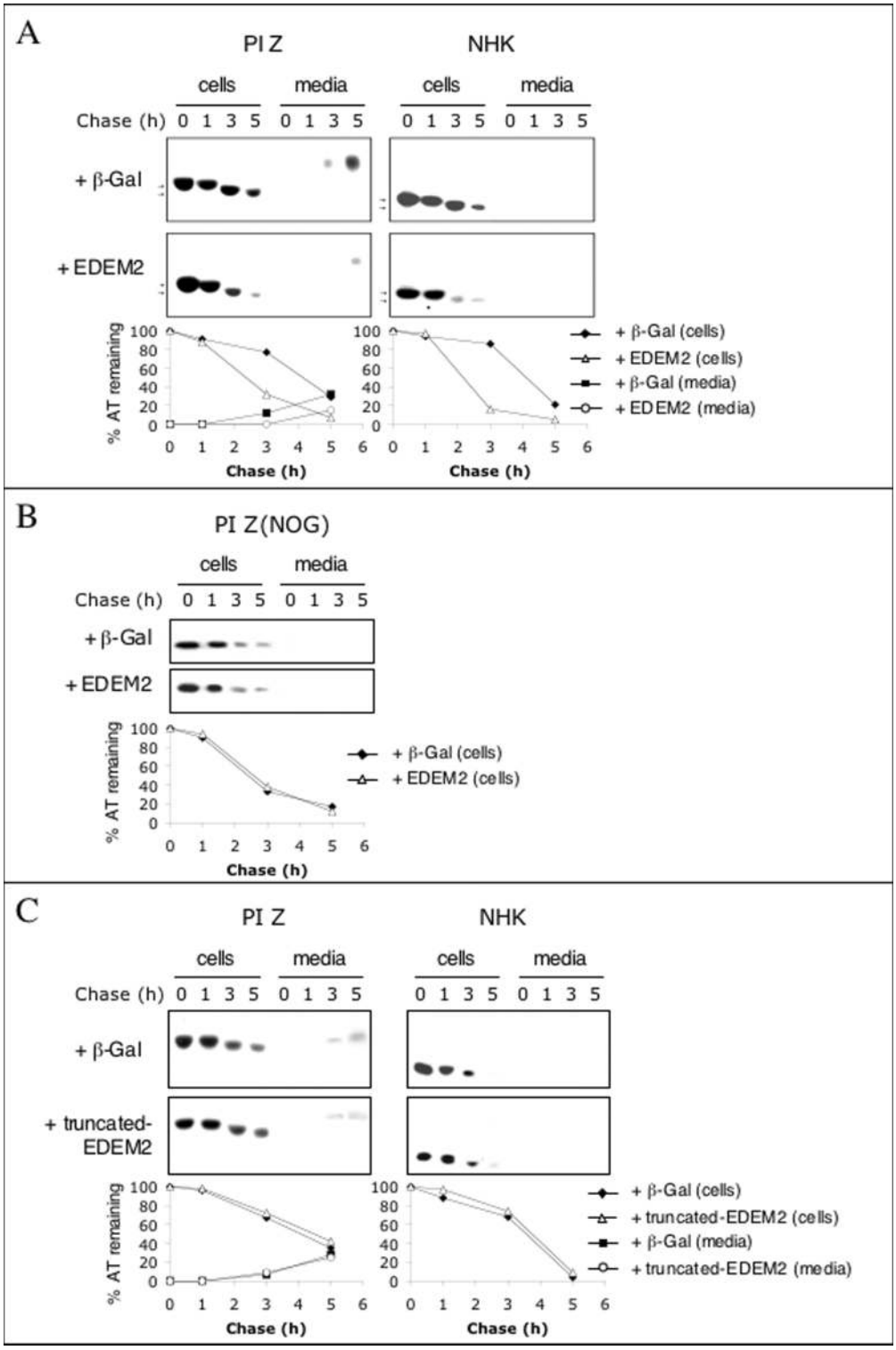

Fig. 9. EDEM2 accelerates degradation of misfolded AT. (**A**) Pulse-chase studies were performed in HEK293 cells that were transiently cotransfected with TCM-EDEM2 (middle panels) and either PI Z or N_{HK}. Control pulse-chase studies employed a β-gal expression construct (top panels) in place of TCM-EDEM2 in combination with either PI Z or N_{HK}. Cells were labeled for 15 min with [^{35}S] Met and chased for the time indicated. Radiolabeled AT was immunoprecipitated from cell lysates or media, separated by SDS–PAGE, and detected by fluorography. Quantification of AT levels are shown below the autoradiograms. (**B**) Similar to **A**, left panels, except that the PI Z expression construct, was replaced with a nonglycosylated PI Z mutant expression construct, PI Z(NOG). The specificity of EDEM2 for accelerating disposal of unfolded glycoproteins was indicated by the lack of enhancement of degradation of a nonglycosylated form of PI Z. (**C**) Similar to **A,** except that the construct encoding truncated EDEM2 was used in place of full-length TCM-EDEM2 in the cotransfections. The full-length TCM-EDEM2 protein was able to accelerate the degradation of N_{HK} and cause acceleration of PI Z disposal, but COOH-terminal truncation of EDEM2 resulted in a protein that was ineffective in enhancing mutant AT disposal.

with the other two homologs. Based on motif searches within the COOH-terminal extensions, the EDEM1 extension contains a putative ATP/GTP-binding site motif A (P-loop) (Falquet *et al.*, 2002), EDEM2 has no recognizable motifs, and EDEM3 has a putative protease-associated domain in the middle of the extended tail (Falquet *et al.*, 2002; Mahon and Bateman, 2000) as well as a COOH-terminal KDEL ER retention motif (Munro and Pelham, 1987).

Although EDEM2 shares sequence similarity with the Class I mannosidases, EDEM2 does not have detectable α-mannosidase activity. In our experiments, the oligosaccharides, $Man_{9-5}GlcNAc_2$, could not be trimmed by recombinant EDEM2. Additionally, the total oligosaccharide profile of labeled cells was the same in cells transfected with EDEM2 compared with untransfected cells (Figure 6). These results are consistent with a previous study in *S. cerevisiae* indicating no change in glycan processing profiles between wild type and Δhtm1/mnl1 strains (Jakob *et al.*, 2001). Similarly, no α-mannosidase activity was detected for mouse EDEM1 (Hosokawa *et al.*, 2001).

The reason why the conserved α-mannosidase homology domains of EDEM2 and other EDEM proteins do not exhibit catalytic activity has yet to be determined. Sequence similarity between EDEM2 and the Class I mannosidases lies predominantly in the α helical segments of the $(\alpha\alpha)_7$ barrel structure (Vallee *et al.*, 2000a,b). Residues within the catalytic site at the core of the $(\alpha\alpha)_7$ barrel also appear to be conserved, whereas conservation in primary sequence is lost in the loop regions connecting the helices (Figure 1C). One potential explanation for the lack of hydrolase activity is that EDEM members lack conserved cysteine residues that form a disulfide bridge between two of the helices in the $(\alpha\alpha)_7$ barrel (Lipari and Herscovics, 1996; Vallee *et al.*, 2000b). However, the *T. reesei* α-1,2-mannosidase also lacks these conserved cysteines residues and is still an active mannosidase, indicating that the disulfide is not essential for hydrolase activity (Van Petegem *et al.*, 2001).

Recombinant expression of EDEM2 in HEK293 cells generated a protein of 70 kDa for TCM-EDEM2 and 64 kDa for truncated EDEM2 (intracellular), as determined by SDS–PAGE (Figure 4). The four N-linked glycosylation sites on EDEM2 are susceptible to complete cleavage by endoglycosidase H, indicating that EDEM2 has a pre-Golgi localization (Figure 5). A large percentage of the truncated construct is secreted, in contrast to full-length EDEM2 that is retained within the cell (Figure 4), indicating that localization of EDEM2 is influenced by the COOH-terminal extension beyond the mannosidase homology domain.

Supporting a role for the EDEM proteins in ERAD, the three human EDEM homologs presumably are localized to the ER, but each by a different mechanism. EDEM1 is predicted to be a type II ER transmembrane protein. EDEM3 contains the COOH-terminal KDEL ER retrieval motif. EDEM2 is predicted to be a soluble protein and has no recognizable ER retention signal but was found to colocalize with the ER marker, calreticulin (Figure 7). EDEM2 contains a hydrophobic sequence at the NH_2-terminus predicted to be a cleavable signal sequence (Figure 1A and 1B), although if this sequence acted as an uncleaved signal anchor it could account for the membrane association and retention. Exchanging the putative cleavable signal from the EDEM2 sequence for the *T. cruzi* α-mannosidase cleavable signal sequence does not alter the localization pattern of EDEM2 by comparison to a COOH-terminal tagged form of the protein that retains the endogenous putative N-terminal signal sequence. This argues against the idea that the hydrophobic sequence at the NH_2-terminus is responsible for ER retention. Although a large percentage of truncated EDEM2 is secreted, the protein that is retained in the cell remains predominantly in an ER localization (Figure 7).

Similar to murine EDEM1 (Hosokawa *et al.*, 2001), EDEM2 is able to interact with the misfolded AT variants N_{HK} and PI Z (Figure 8). The interaction with the substrate most likely includes a glycan component, as demonstrated by the ability to accelerate the degradation of glycosylated AT mutants but not a nonglycosylated mutant of AT (Figure 9). In contrast to the observation that the full-length form of EDEM2 (TCM-EDEM2) was able to accelerate the degradation of the misfolded AT variants, the COOH-terminal truncation beyond the mannosidase-homology domain eliminated the ability of EDEM2 to accelerate mutant AT degradation. One possible explanation for these data is that the COOH-domain has a role in the interaction with other proteins in the ERAD pathway and that truncation of the COOH-terminus interferes with this function.

We noted that the degradation of the AT variant N_{HK} occurs more quickly than for PI Z. One explanation for the delayed rate of disposal for PI Z is the ability of this mutant to spontaneously generate loop-sheet polymers that may reduce the accessibility of protein monomers to be targeted for degradation (Lomas *et al.*, 1992). Although the rate of polymerization has been reported to be low in HEK293 cells (Cabral *et al.*, 2002), aggregate formation could still influence the rate of entry into the disposal machinery.

The mobility shift of radiolabeled AT in SDS–PAGE was found to increase during the chase period and is complete by 3 h chase (Figure 9). This shift to a lower apparent molecular mass is consistent with glycan processing and is coincident with disposal of the radiolabeled protein. This is in agreement with the current model of ERAD where ER mannosidase I trimming of $Man_9GlcNAc_2$ structures to $Man_8GlcNAc_2$ generates the glycan signal for degradation. The data would also be consistent with the recent data indicating that further processing to $Man_{7-5}GlcNAc_2$ structures may be the alternate glycan signal in mammalian cells (Ermonval *et al.*, 2001; Frenkel *et al.*, 2003; Hosokawa *et al.*, 2003; Kitzmuller *et al.*, 2003).

In summary, EDEM2 is localized in the ER where it was able to bind to the AT variants and accelerate their degradation. The differences in sequence between the EDEM homologs suggest overlapping but specific roles for each member. In characterizing this subfamily, the role of the COOH-extension after the mannosidase homology domain will be a major factor in determining the mechanism of action. For EDEM2, the COOH-terminal extension appears to be involved in both ER retention and in the degradation of substrates. For EDEM1, its role in ERAD may involve a transfer of misfolded proteins from calnexin to the putative lectin. Whether the other homologs follow this pathway is unknown. Because the present model of EDEM1 interaction with calnexin is through its transmembrane domain,

the fact that EDEM2 and EDEM3 are proposed to be soluble proteins would suggest that a similar mechanism for interaction with calnexin is not likely to pertain for these latter proteins. Finally, establishing the nature of the lectin activity for the EDEM homologs needs to be further characterized, because a direct role of a specific glycan structure in the initiation or maintenance of the interaction remains to be demonstrated.

Materials and methods

Computer analysis

Multiple sequence alignment was performed by ClustalW 1.6. Preparation of an unrooted neighbor-joining phylogenetic tree was performed with TreeView PPC (1.6.6). Kyte-Doolittle hydropathy plot was created by subroutines from the Genetics Computer Group (Madison, WI). Interpolation of molecular weight from SDS–PAGE was performed by Quantity One version 4.3.0 software (Bio-Rad, Hercules, CA).

Isolation of EDEM2 and generation of full-length and truncated fusion protein constructs

Mouse Golgi mannosidase IA (GenPept AAA17747.1) was used to query human expressed sequence tag (EST) sequences using the translated BLAST (tblastn) algorithm in the NCBI database (Altschul *et al*., 1990). Several partial novel sequences were identified. Based on sequence comparison to other family 47 glycosidases, the sequence of EDEM2 was not complete at the 5′ end. 5′-Rapid amplification of cDNA ends (RACE) was used to isolate the remainder of the coding region, using a cDNA preparation from human spleen mRNA as the template. Primers for 5′-RACE were based on the sequence from the human EST R67182. The resulting 270-bp RACE product was isolated, subcloned into the pCR2.1 cloning vector (Invitrogen, Carlsbad, CA), and sequenced.

The full-length coding sequence of EDEM2 was generated by amplification from a human pancreas cDNA source (Marathon Ready cDNA, Clontech, Palo Alto, CA), subcloned into the pCR2.1 vector, and sequenced. A full-length EDEM2 construct with a COOH-terminal epitope tag was also made. To generate an in-frame fusion with the vector-encoded COOH-terminal tag, full-length EDEM2 in the pcDNA3.1/Myc-His vector (Invitrogen) was altered by site-directed mutagenesis using the QuikChange site-directed mutagenesis kit (Stratagene, La Jolla, CA) to change the stop codon, UAA, to a Leu codon, CTA. The resulting construct (EDEM2-Myc-His/pcDNA3.1) encodes a polypeptide containing four amino acids (LSFL) between the coding region and the vector encoded Myc epitope and 6× His peptide.

AnHA epitope was also added to the COOH-terminus of the EDEM2-Myc-His construct at a Sal I restriction site between the myc epitope and His tag. Sense and antisense oligonucleotides containing a 2× HA epitope sequence flanked by Sal I sites were synthesized (Molecular Genetics Instrumentation facility, University of Georgia), phosphorylated with T4 DNA kinase, mixed at 95°C, and allowed to cool gradually. The annealed oligonucleotides were ligated with the Sal I-cut expression vector and sequenced to confirm the proper insertion of the HA tag (EDEM2-Myc-HA-His/pEAK).

To generate a construct without the putative signal sequence, a human pancreas cDNA source was used as the template for PCR. The primers were designed to amplify the EDEM2 coding region from amino acid 18 to the stop codon, with a SmaI site at the 5′ end of the coding region. The resulting 1.7-kb amplimer was subcloned into the pCR2.1 vector and sequenced. Insertion into this vector placed a Not I site downstream of the stop codon. The putative signal sequence of EDEM2 was replaced by the following sequence: a 5′ Hind III restriction site followed by the 5′ untranslated region and NH_2-terminal signal sequence of TCM (GenBank accession number AF077741), a 10× His tag, a 2× HA epitope, and a Sma I site at the 3′ end of the sequence. A Hind III/SmaI fragment containing the TCM signal sequence and the tag sequences and a SmaI/Not I fragment containing EDEM2 (residues 18–578) were both inserted into a Hind III/Not I cut pEAK 10 vector (Edge Biosystems, Gaithersburg, MD) creating TCM-EDEM2/pEAK.

For expression of truncated EDEM2, the EDEM2 coding region was altered by site directed mutagenesis as described to introduce a stop codon after amino acid 492, 10 amino acids after the end of the mannosidase homology domain. A restriction fragment (EcoRV/HindIII) containing the mutated region was swapped into the TCM-EDEM2/pEAK construct to create a construct that expressed the TCM-His-HA tag and the mannosidase homology domain sequence but not the COOH-terminal extension beyond the homology region (truncated EDEM2/pEAK).

Northern blot analysis

Northern blots containing poly(A+) RNA from various human tissues were purchased from Clontech Laboratories. The blots were prehybridized, hybridized, and washed as described previously (Moremen and Robbins, 1991), using a 1-kb PCR amplimer derived from the EDEM2 coding region as a radiolabeled probe. The blots were subsequently hybridized with a ^{32}P-labeled human-actin control probe (Clontech) to act as an RNA load control. Blots were visualized with a PhosphorImager (Molecular Dynamics, Sunnyvale, CA) after a 1-day exposure.

Generation of stably and transiently transfected HEK293 cells

For stable expression, HEK293 cells were grown to 40% confluency in T-75 flasks (Corning, Corning, NY) and transfected by the calcium phosphate method (Sambrook *et al*., 1989). Briefly, EDEM2 constructs (15 μg) were mixed with calcium phosphate and added to the cell monolayer in fresh Dulbecco's modified Eagle's medium (DMEM)/10% fetal calf serum (FCS) (Sigma, St. Louis, MO). Cells were incubated for 6 h at 37°C. The medium was then replaced, and cells were grown an additional 24 h followed by selection with 0.5 μg/ml puromycin. During subsequent passages, the puromycin was increased to a final concentration of 2 μg/ml. Mock-transfected HEK293 cells were used as a negative control for puromycin selection.

N_{HK} (Sifers *et al.*, 1988), PI Z (Le *et al.*, 1992), and deglycosylated (Samandari and Brown, 1993) variants of AT were generated by site-directed mutagenesis of the wild type AT cDNA (GenBank accession number NM 000295) as described and subcloned into pcDNA3.1/Zeo (Invitrogen). The nonglycosylated form of PI Z, PIZ(NOG), was generated using site-directed mutagenesis by altering Nx(S/T) sites to Qx(S/T). For stable expression, PI Z/pcDNA3.1 or N_{HK}/pcDNA3.1 was transfected into HEK293 cells in the same manner as the pEAK vector constructs and selected with 200 μg/ml zeocin.

For transient transfection, cells were grown to 70% confluency in 100-mm dishes prior to transfection by the Lipofectamine 2000 method (Invitrogen) according to the method of Wu *et al*. (2003). Each transfection cocktail consisted of 30 μg DNA and included combinations of PI Z/pCDNA3.1, N_{HK}/pCDNA3.1, pSV-β-galactosidase Control Vector (Promega, Madison, WI), PI Z(NOG)/pCDNA3.1, TCM-EDEM2/pEAK, and truncated EDEM2/pEAK. Cells were collected 48 h posttransfection, mixed, and subcultured at identical cell densities in either 60-mm or 100-mm dishes to eliminate differences in transfection efficiency.

Expression in suspension culture

For purification of EDEM2, stably transfected pEAK cells were grown in 1 L suspension culture (1×10^6 cells/ml) using SFM II media (Gibco, Grand Island, NY) supplemented with 0.2 μg/ml puromycin. The cells were harvested and washed in 50 mM Na-2-(*N*-morpholino)ethanesulfonic acid (MES) (pH 7). Cells were resuspended in lysis buffer (50 mM Na-MES, 375 mM NaCl, 1% Triton X-100, 20 mM imidazole, 1 mM $CaCl_2$, pH 6.3) supplemented with 1 mM phenylmethylsulfonyl fluoride (Sigma) and 1× ethylenediamine tetra-acetic acid free Complete Protease Inhibitor cocktail (Roche, Indianapolis, IN). Cells were lysed in a glass-Teflon homogenizer for 1 min, and the lysate was centrifuged at $31{,}000 \times g$ for 15 min. The supernatant was loaded onto a 4 ml column of Ni^{2+}-NTA resin (Qiagen, Valencia, CA), and the column was washed with 60 ml lysis buffer, followed by elution using a 100 ml imidazole gradient (50–400 mM) containing 100 mM Na-MES, 150 mM NaCl, 1 mM $CaCl_2$ (pH 6.3). The samples were resolved by SDS–PAGE and immunoblotted with mouse anti-HA antibody (1:5000) (Covance, Berkeley, CA) followed by the goat anti-mouse-alkaline phosphatase-conjugated antibody (1:5000) (Promega). The relevant fractions were pooled and dialyzed.

N-glycanase and endoglycosidase H digest of EDEM2

HEK293 cells transfected with TCM-EDEM2, EDEM2-Myc-HA-His, or truncated EDEM2 were labeled for 2 h with ^{35}S-Met/Cys and chased for 3 h. Cell lysates and media were immunoprecipitated as will be described with an antibody to HA. The samples were heated at 90°C for 5 min in 50 mM Tris (pH 7), SDS (0.25%), and β-mercaptoethanol (0.1 M). For N-glycanase digests, the solutions were cooled to room temperature, diluted with an equal volume of 500 mM Tris (pH 7), 5% NP-40, followed by a 14-h incubation at 37°C with ~ 2 U N-glycanase (gift from Dr. Michael Pierce, University of Georgia). For endoglycosidase H digests, 1/10 volume of 0.5 M Na-citrate (pH 5.5) was added, followed by a 2-h incubation at 37°C with 500 U endoglycosidase H (Roche). A mock digest was also performed. The samples were resolved by SDS–PAGE and visualized by autoradiography.

Substrate assays

Oligosaccharide substrates were obtained, and assays were performed essentially as described previously (Lal *et al.*, 1998). PA-tagged $Man_9GlcNAc_2$, $Man_8GlcNAc_2$ (isomers A, B, and C), $Man_6GlcNAc_2$, or $Man_5GlcNAc_2$ were each incubated for 2–10 h at 37°C with Ni^{2+}-NTA purified EDEM2 in a buffer of 50 mM Na-MES (pH 7), 1 mM $CaCl_2$. As a positive control, recombinant human ER mannosidase I or Golgi mannosidase IA was added into a sample of EDEM2 (Gonzalez *et al.*, 1999; Lal *et al.*, 1998). The digestion products were resolved on a Hypersil APS-2 NH_2 HPLC column as previously described (Lal *et al.*, 1998).

Oligosaccharide labeling and preparation

Labeling with [^{3}H]mannose was performed as described previously (Tabas and Kornfeld, 1980). Briefly, cells were labeled with 1 mCi [^{3}H]mannose in DMEM for 30 min and then chased for 30 min in unlabeled DMEM. Cell lysates were prepared by addition of 1% SDS, Na-succinate, pH 5.5, to the phosphate buffere salined (PBS)-washed cell pellets. The samples were incubated at 80°C for 5 min, followed by sonication. Glycoproteins were isolated by acetone precipitation, and the pellet was resuspended in 50 mM Na-citrate, pH 5.5, for endoglycosidase H digestion (3000 U, 2 h, 37°C). A second acetone precipitation was performed to separate the released N-linked oligosaccharides from proteins. The N-linked oligosaccharide fraction was dried and resuspended in 5% acetic acid. For separation from detergents, the samples were run on an HLB 3cc cartridge (Waters). Prior to sample application the HLB cartridge was activated with methanol and washed with 5% acetic acid. After application of the sample, the cartridge was washed with 5% acetic acid, and the material that ran through the column with the load and wash fractions was collected. The sample was dried, resuspended in 10 mM ammonium bicarbonate, and desalted on a Sephadex G-15 column. The oligosaccharides were PA-tagged as previously described (Hase 1994; Lal *et al.*, 1998), desalted over a Sephadex G-15 column, and resolved on a Hypersil APS-2 NH_2 HPLC column using PA-tagged $Man_{9-5}GlcNAc_2$ as the standards. The oligosaccharides were resolved on NH_2 HPLC using the following conditions: isocratic flow (0.8 ml/min) in a buffer containing 57% 100 mM Na-phosphate buffer, pH 4, and 43% acetonitrile.

IF microscopy

Stably transfected HEK293 cells were grown in DMEM/10% FCS on eight-well chamber slides (Lab-Tek, Nalge Nunc, Rochester, NY) coated with 0.01% poly-L-lysine (Sigma). Slides were washed in PBS and fixed with 3.5% formaldehyde in 100 mM potassium phosphate (pH 7) for 15 min at 37°C. Following fixation, the cells were washed with PBS and permeabilized by incubation with 0.2% saponin and 10% FCS in PBS (buffer A) for 15 min at 37°C. Primary antibodies (mouse anti-HA monoclonal antibody,

Covance, 1:1000; mouse anti-Myc monoclonal antibody, Invitrogen, 1:1000; rabbit anti-calreticulin polyclonal antibody, Affinity Bioreagents (Golden, CO), 1:1000; rabbit anti-human Golgi Man II polyclonal antibody, generated in Moremen lab to recombinant human Golgi Man II, unpublished, 1:1000; rabbit anti-cytosolic mannosidase polyclonal antibody generated in Moremen lab to recombinant rat cytosolic mannosidase, unpublished, 1:1000; or rabbit anti-MEK-1 polyclonal antibody, Santa Cruz Biotechnology, Santa Cruz, CA, 1:1000) diluted in buffer A were incubated with the chamber slides for 1 h at room temperature, followed by several washes with PBS. Secondary antibody (Alexafluor anti-mouse 594,Molecular Probes, Eugene, OR, 1:1000; and Alexafluor anti-rabbit 488, Molecular Probes, 1:1000) incubations were also for 1 h at room temperature followed by several washes with PBS. The slides were then mounted in Permafluor mounting media (Immunon Thermo Shandon, West Palm Beach, FL) and viewed with a Leica DM IRE2 microscope or Bio-Rad MRC-600 laser scanning confocal microscope.

IP of recombinant EDEM2 from HEK293 cells

Cells were incubated in Met/Cys-free DMEM/5% dialyzed FCS for 30 min and labeled with [^{35}S]-Met/Cys (ICN, Irvine, CA) for 2 h. Cells were harvested and collected by centrifugation and lysed by vortexing in a buffer containing 2% CHAPS, HEPES buffered saline (HBS), pH 7.6. Before IP, cell lysates were centrifuged at 22,000 × *g* for 20 min, followed by incubation with 60 µl Protein A-agarose (Repligen, Waltham, MA) for 1 h and centrifugation at 3000 × *g* to preclear the lysate. The primary antibodies for the IP were prebound to a separate aliquot of Protein A-agarose resin and before IP unbound antibody was removed by washing with PBS. Controls containing Protein A-agarose with nonspecific antibody were included for each cell line. The precleared cell lysates were added to the Protein A-agarose-antibody complex and incubated at 4°C overnight. The resin was washed three times with 0.5% CHAPS, HBS (pH 7.6), and once in 50 mM Na-HEPES (pH 7) before elution by boiling in SDS sample buffer. Samples were run on SDS–PAGE and visualized by autoradiography.

Metabolic radiolabeling and IP of AT

Metabolic radiolabeling was preceded by a 30-min incubation at 37°C in Met-free DMEM (ICN) containing 10% FCS prior to a 15-min pulse with [^{35}S] Met (Easy Tag Express Mix, Perkin Elmer Life Sciences, Boston, MA) as described (Le *et al*., 1998). Monolayers were washed with Dulbecco's OBS (Gibco) to remove unincorporated radiolabel and then chased for the desired period at 37°C with Met-free starvation medium supplemented with a 10-fold excess of unlabeled methionine. Cells were lysed and collected by scraping in buffered NP-40 detergent (Calbiochem, San Diego, CA) at 4°C. Media were collected at each time point and adjusted to 0.5% NP-50. For IP, all samples were cleared by centrifugation (3000 × *g*, 5 min, 4°C) prior to receiving an excess of goat anti human AT (Ig fraction, ICN), and then incubated for 2 h with constant rotation at 4°C. Immunocomplexes were washed as previously described (Le *et al*., 1998) prior to resolution by SDS–PAGE and detection by fluorographic enhancement of the vacuum-dried gels (Cabral *et al*., 2002; Le *et al*., 1998). Quantitative analysis was performed by densitometric scanning (NIH IMAGE program).

Acknowledgments

We gratefully acknowledge members of the Moremen laboratory and Dr. Gerardo Alvarez-Manilla for assistance and discussions during the course of these studies. We thank the Molecular Genetics Instrumentation Facility at the University of Georgia for DNA sequencing and oligonucleotide synthesis. We also express our thanks to Dr. J. Michael Pierce for supplying the N-glycanase for our studies. This work was supported by NIH Research Grants GM47533 and RR05351 (to K.W.M.) and HL62553, R01 DK064232, and R01 HL62553 (to R.N.S.); by the Alpha1-Foundation Research Grants #R02-5, #1Y102-6, and #F03-12 (to R.N.S.); and by the Fernandez Liver Research Initiative from the Alpha1-Foundation Grant #1Y102-6.

Abbreviations

AT, α1-antitrypsin; DMEM, Dulbecco's modified Eagle's medium; EDEM, ER degradation–enhancing α-mannosidase-like protein; ER, endoplasmic reticulum; ERAD, ER-associated degradation; EST, expressed sequence tags; FCS, fetal calf serum; HA, hemagglutinin; HBS, HEPES-buffered saline; HPLC, high-performance liquid chromatography; IF, immunofluorescence; IP, immunoprecipitation; MES, 2-(*N*-morpholino)ethanesulfonic acid; NTA, nitrilotriacetic acid; PA, pyridylamine; PBS, phosphate buffered saline; PCR, polymerase chain reaction; RACE, rapid amplification of cDNA ends; SDS–PAGE, sodium dodecyl sulfate–polyacrylamide gel electrophoresis; TCM, *T. cruzi* lysosomal α-mannosidase; UPR, unfolded protein response.

References

Altschul, S.F., Gish, W., Miller, W., Myers, E.W., and Lipman, D.J. (1990) Basic local alignment search tool. *J. Mol. Biol.*, **215**, 403–410.

Cabral, C.M., Liu, Y., and Sifers, R.N. (2001) Dissecting glycoprotein quality control in the secretory pathway. *Trends Biochem. Sci.*, **26**, 619–624.

Cabral, C.M., Liu, Y., Moremen, K.W., and Sifers, R.N. (2002) Organizational diversity among distinct glycoprotein endoplasmic reticulum-associated degradation programs. *Mol. Biol. Cell*, **13**, 2639–2650.

Ellgaard, L. and Helenius, A. (2001) ER quality control: towards an understanding at the molecular level. *Curr. Opin. Cell Biol.*, **13**, 431–437.

Ellgaard, L. and Helenius, A. (2003) Quality control in the endoplasmic reticulum. *Nat. Rev. Mol. Cell Biol.*, **4**, 181–191.

Ermonval, M., Kitzmuller, C., Mir, A.M., Cacan, R., and Ivessa, N.E. (2001) N-glycan structure of a short-lived variant of ribophorin I expressed in the MadIA214 glycosylation-defective cell line reveals the role of a mannosidase that is not ER mannosidase I in the process of glycoprotein degradation. *Glycobiology*, **11**, 565–576.

Falquet, L., Pagni, M., Bucher, P., Hulo, N., Sigrist, C. J., Hofmann, K., and Bairoch, A. (2002) The PROSITE database, its status in 2002. *Nucleic Acids Res.*, **30**, 235–238.

Flierman, D., Ye, Y., Dai, M., Chau, V., and Rapoport, T.A. (2003) Polyubiquitin serves as a recognition signal, rather than a ratcheting molecule, during retrotranslocation of proteins across the endoplasmic reticulum membrane. *J. Biol. Chem.*, **278**, 34774–34782.

Frenkel, Z., Gregory, W., Kornfeld, S., and Lederkremer, G.Z. (2003) Endoplasmic reticulum-associated degradation of mammalian glycoproteins involves sugar chain trimming to Man6-5GlcNAc2. *J. Biol. Chem.*, **278**, 34119–34124.

Gonzalez, D.S., Karaveg, K., Vandersall-Nairn, A.S., Lal, A., and Moremen, K.W. (1999) Identification, expression, and characterization of a cDNA encoding human endoplasmic reticulum mannosidase I, the enzyme that catalyzes the first mannose trimming step in mammalian Asn-linked oligosaccharide biosynthesis. *J. Biol. Chem.*, **274**, 21375–21386.

Hase, S. (1994) High-performance liquid chromatography of pyridylaminated saccharides *Methods Enzymol.*, **230**, 225–237.

Hirokawa, T., Boon-Chieng, S., and Mitaku, S. (1998) SOSUI: classification and secondary structure prediction system for membrane proteins. *Bioinformatics*, **14**, 378–379.

Hosokawa, N., Wada, I., Hasegawa, K., Yorihuzi, T., Tremblay, L.O., Herscovics, A., and Nagata, K. (2001) A novel ER alpha-mannosidase-like protein accelerates ER-associated degradation. *EMBO Rep.*, **2**, 415–422.

Hosokawa, N., Tremblay, L.O., You, Z., Herscovics, A., Wada, I., and Nagata, K. (2003) Enhancement of endoplasmic reticulum (ER) degradation of misfolded Null Hong Kong alpha1-antitrypsin by human ER mannosidase I. *J. Biol. Chem.*, **278**, 26287–26294.

Jakob, C.A., Burda, P., Roth, J., and Aebi, M. (1998) Degradation of misfolded endoplasmic reticulum glycoproteins in *Saccharomyces cerevisiae* is determined by a specific oligosaccharide structure. *J. Cell Biol.*, **142**, 1223–1233.

Jakob, C.A., Bodmer, D., Spirig, U., Battig, P., Marcil, A., Dignard, D., Bergeron, J.J., Thomas, D.Y., and Aebi, M. (2001) Htm1p, a mannosidase-like protein, is involved in glycoprotein degradation in yeast. *EMBO Rep.*, **2**, 423–430.

Jarosch, E., Lenk, U., and Sommer, T. (2003) Endoplasmic reticulum-associated protein degradation. *Int. Rev. Cytol.*, **223**, 39–81.

Kitzmuller, C., Caprini, A., Moore, S.E., Frenoy, J.P., Schwaiger, E., Kellermann, O., Ivessa, N.E., and Ermonval, M. (2003) Processing of N-linked glycans during the endoplasmic reticulum associated degradation of a short-lived variant of ribophorin I. *Biochem. J.*, **376**, 687–696.

Kostova, Z. and Wolf, D.H. (2003) For whom the bell tolls: protein quality control of the endoplasmic reticulum and the ubiquitin-proteasome connection. *EMBO J.*, **22**, 2309–2317.

Kyte, J. and Doolittle, R.F. (1982) A simple method for displaying the hydropathic character of a protein. *J. Mol. Biol.*, **157**, 105–132.

Lal, A., Pang, P., Kalelkar, S., Romero, P.A., Herscovics, A., and Moremen, K.W. (1998) Substrate specificities of recombinant murine Golgi alpha1, 2-mannosidases IA and IB and comparison with endoplasmic reticulum and Golgi processing alpha1,2-mannosidases. *Glycobiology*, **8**, 981–995.

Le, A., Ferrell, G.A., Dishon, D.S., Le, Q.Q., and Sifers, R.N. (1992) Soluble aggregates of the human PiZ alpha 1-antitrypsin variant are degraded within the endoplasmic reticulum by a mechanism sensitive to inhibitors of protein synthesis. *J. Biol. Chem.*, **267**, 1072–1080.

Lipari, F. and Herscovics, A. (1996) Role of the cysteine residues in the alpha1,2-mannosidase involved in N-glycan biosynthesis in *Saccharomyces cerevisiae*. The conserved Cys340 and Cys385 residues form an essential disulfide bond. *J. Biol. Chem.*, **271**, 27615–27622.

Liu, Y., Choudhury, P., Cabral, C.M., and Sifers, R.N. (1999) Oligosaccharide modification in the early secretory pathway directs the selection of a misfolded glycoprotein for degradation by the proteasome. *J. Biol. Chem*, **274**, 5861–5867.

Lomas, D.A., Evans, D.L., Finch, J.T., and Carrell, R.W. (1992) The mechanism of Z alpha 1-antitrypsin accumulation in the liver. *Nature*, **357**, 605–607.

Mahon, P. and Bateman, A. (2000) The PA domain: a protease-associated domain. *Protein Sci.*, **9**, 1930–1934.

Mancini, R., Aebi, M., and Helenius, A. (2003) Multiple ER-associated pathways degrade mutant yeast carboxypeptidase Y in mammalian cells. *J. Biol. Chem.*, **278**, 46895–46905.

McCracken, A.A. and Brodsky, J.L. (2003) Evolving questions and paradigm shifts in endoplasmic-reticulum-associated degradation (ERAD). *Bioessays*, **25**, 868–877.

Molinari, M., Calanca, V., Galli, C., Lucca, P., and Paganetti, P. (2003) Role of EDEM in the release of misfolded glycoproteins from the calnexin cycle. *Science*, **299**, 1397–1400.

Moremen, K.W. and Robbins, P.W. (1991) Isolation, characterization, and expression of cDNAs encoding murine alpha-mannosidase II, a Golgi enzyme that controls conversion of high mannose to complex N-glycans. *J. Cell Biol.*, **115**, 1521–1534.

Munro, S. and Pelham, H.R. (1987) A C-terminal signal prevents secretion of luminal ER proteins. *Cell*, **48**, 899–907.

Nakatsukasa, K.N.S., Hosokawa, N., Nagata, K., and Endo, T. (2001) Mnl1p, an alpha-mannosidase-like protein in yeast *Saccharomyces cerevisiae*, is required for endoplasmic reticulum-associated degradation of glycoproteins. *J. Biol. Chem.*, **276**, 8635–8638.

Oda, Y., Hosokawa, N., Wada, I., and Nagata, K. (2003) EDEM as an acceptor of terminally misfolded glycoproteins released from calnexin. *Science*, **299**, 1394–1397.

Parfrey, H., Mahadeva, R., and Lomas, D.A. (2003) Alpha(1)-antitrypsin deficiency, liver disease and emphysema. *Int. J. Biochem. Cell Biol.*, **35**, 1009–1014.

Samandari, T. and Brown, J.L. (1993) A study of the effects of altering the sites for N-glycosylation in alpha-1-proteinase inhibitor variants M and S. *Protein Sci.*, **2**, 1400–1410.

Sambrook, J., Fritsch, E.F. and Maniatis, T. (1989) *Molecular cloning: a laboratory manual*. Cold Spring Harbor Laboratory Press, Cold Spring Harbor, NY.

Sifers, R.N., Brashears-Macatee, S., Kidd, V.J., Muensch, H., and Woo, S.L. (1988) A frameshift mutation results in a truncated alpha 1-antitrypsin that is retained within the rough endoplasmic reticulum. *J. Biol. Chem.*, **263**, 7330–7335.

Tabas, I. and Kornfeld, S. (1980) Biosynthetic intermediates of beta-glucuronidase contain high mannose oligosaccharides with blocked phosphate residues. *J. Biol. Chem.*, **255**, 6633–6639.

Trombetta, E.S. and Parodi, A.J. (2003) Quality control and protein folding in the secretory pathway. *Annu. Rev. Cell Dev. Biol.*, **19**, 649–676.

Tsai, B., Ye, Y., and Rapoport, T.A. (2002) Retro-translocation of proteins from the endoplasmic reticulum into the cytosol. *Nat. Rev. Mol. Cell Biol.*, **3**, 246–255.

Vallee, F., Karaveg, K., Herscovics, A., Moremen, K.W., and Howell, P.L. (2000a) Structural basis for catalysis and inhibition of N-glycan processing class I alpha 1,2-mannosidases. *J. Biol. Chem.*, **275**, 41287–41298.

Vallee, F., Lipari, F., Yip, P., Sleno, B., Herscovics, A., and Howell, P.L. (2000b) Crystal structure of a class I alpha1,2-mannosidase involved in N-glycan processing and endoplasmic reticulum quality control. *EMBO J.*, **19**, 581–588.

Vandersall-Nairn, A.S., Merkle, R.K., O'Brien, K., Oeltmann, T.N., and Moremen, K.W. (1998) Cloning, expression, purification, and characterization of the acid alpha-mannosidase from *Trypanosoma cruzi*. *Glycobiology*, **8**, 1183–1194.

Van Petegem, F., Contreras, H., Contreras, R., and Van Beeumen, J. (2001) *Trichoderma reesei* alpha-1,2-mannosidase: structural basis for the cleavage of four consecutive mannose residues. *J. Mol. Biol.*, **312**, 157–165.

Wu, Y., Swulius, M.T., Moremen, K.W., and Sifers, R.N. (2003) Elucidation of the molecular logic by which misfolded alpha 1-antitrypsin is preferentially selected for degradation. *Proc. Natl Acad. Sci. USA*, **100**, 8229–8234.

Yang, M., Omura, S., Bonifacino, J.S., and Weissman, A.M. (1998) Novel aspects of degradation of T cell receptor subunits from the endoplasmic reticulum (ER) in T cells: importance of oligosaccharide processing, ubiquitination, and proteasome-dependent removal from ER membranes. *J. Exp. Med.*, **187**, 835–846.

Ye, Y., Meyer, H.H., and Rapoport, T.A. (2003) Function of the p97-Ufd1-Npl4 complex in retrotranslocation from the ER to the cytosol: dual recognition of nonubiquitinated polypeptide segments and polyubiquitin chains. *J. Cell Biol.*, **162**, 71–84.

Yoshida, Y. (2003) A novel role for N-glycans in the ERAD system. *J. Biochem (Tokyo)*, **134**, 183–190.

Yoshida, H., Matsui, T., Hosokawa, N., Kaufman, R.J., Nagata, K., and Mori, K. (2003) A time-dependent phase shift in the mammalian unfolded protein response. *Dev. Cell*, **4**, 265–271.